Liquid-Phase Sintering of SiC-Based Ceramics

V.A. Izhevskyi[1], L.A. Genova[1], J.C. Bressiani[1] and A.H.A. Bressiani[2]

[1] Energéticas e Nucleares, Instituto de Pesquisas, P.O.Box 11049,
CEP 05422-970 São Paulo SP, Brazil

[2] Department of Materials Engineering, Energy and Nuclear Research Institute, Pinheiros,
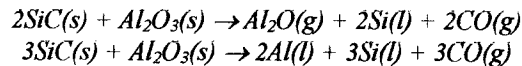C.P. 11049 São Paulo 05422-970, Brazil

Abstract: Microstructural development and phase formation processes during sintering of silicon carbide based materials with AlN and Y_2O_3 sintering additives were investigated. Densification of the materials occurred by liquid-phase sintering mechanism. Proportion of $\alpha-$ and $\beta-$SiC powders in the initial mixtures was a variable parameter. Shrinkage behavior during sintering in interrelation with the starting composition of the material and the sintering atmosphere was investigated by differential dilatometry. Transformation-controlled grain growth mechanism similar to the one observed for silicon nitride based ceramics was established. Evolution of microstructure and phase composition was followed up by scanning electron microscopy and x-ray diffraction, respectively. Possibility of in-situ platelet reinforced dense SiC-based ceramics fabrication with improved mechanical properties by means of sintering was shown.

Introduction

Silicon carbide is considered to be an important structural ceramic material because of a promising combination of properties, such as high oxidation resistance, good mechanical properties retained to high temperatures, high wear resistance, good thermal shock resistance due to high thermal conductivity, etc. All these properties are inherent to silicon carbide due to highly covalent bonding. The latter, however, causes complications with sintering of SiC-based ceramics to high densities, which disadvantage is characteristic for all non-oxide covalent compounds, such as Si_3N_4 and AlN.

Unlike the aforementioned compounds, which tend to decompose severely at high temperatures, silicon carbide can be densified by solid-state sintering process at high temperatures of about 2100^0C with the aid of B and C [1], which dramatically improve the shrinkage kinetics. However, thus sintered materials have poor or, at the best, moderate mechanical properties (flexural strength of 300-450 MPA and fracture toughness of 2.5-4 $MPa \cdot m^{-1/2}$). Liquid-phase sintering of SiC can be achieved at much lower temperatures ($1800-1900^0C$) [2, 3] with the aid of metal oxides, such as Al_2O_3, Y_2O_3, and other rare-earth oxides [4-8]. The densification of SiC by liquid-phase sintering lately draws more attention because the materials processed by this method exhibit superior mechanical properties. The liquid phase sintering of SiC is somewhat similar to the same process for Si_3N_4. The oxide sintering aids react with SiO_2, which is always present at the surface of SiC particles, forming an oxide melt and enhancing densification. However, oxides interact with SiC with massive gaseous products formation leading to high weight loss and porosity [9, 10]. It is known that alumina may interact with silicon carbide according to the following reactions [4]:

$$SiC\ (s)\ +\ Al_2O_3(s)\ \rightarrow Al_2O(g)\ +\ SiO(g)\ +\ CO(g)$$

$$2SiC(s) + Al_2O_3(s) \rightarrow Al_2O(g) + 2Si(l) + 2CO(g)$$
$$3SiC(s) + Al_2O_3(s) \rightarrow 2Al(l) + 3Si(l) + 3CO(g)$$

These reactions occur more actively with the increase of alumina content and the temperature of sintering. These reactions can be to some extent suppressed by the application of the high external partial pressure of CO and/or application of reactive powder beds [4]. However, such an approach is not completely effective and enables to achieve the final density not higher than 98% of theoretical density. Moreover, such techniques are costly and do not guarantee the reproducibility of materials properties.

Additional weight loss occurs during sintering of SiC with Al_2O_3 – Y_2O_3 sintering additives occurs due to the reaction between SiC and SiO_2 surface films:

$$2SiO_2(s) + SiC(s) \rightarrow 3SiO(g) + CO(g)$$
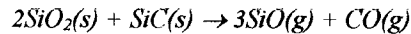
It is therefore obvious that an alternative combination of sintering additives, which will eliminate or reduce the above-mentioned effects determined for densification, will be the best possible solution. As it was suggested by Chia et al [11], aluminum nitride, AlN, in combination with yttria, Y_2O_3, may present a solution. However, this possibility was not investigated in detail and only a limited amount of information is available [11, 12]. Which is of additional interest, due to certain structural similarities SiC and AlN produce solid solutions and formation of mixed crystalline structures was observed [13-17].

By analogy with silicon nitride, it seems to be possible to tailor the microstructure and the structure-sensitive properties of silicon carbide based ceramics by varying α– to β–SiC ratio in the initial mixtures. If α–SiC is used as a starting powder, the final material is characterized by fine homogeneous microstructure with uniaxial grains [5, 18], which results in moderate fracture toughness. Additions of β–SiC in combination with some specially developed thermal treatment leads to in-situ platelet reinforced material formation with improved mechanical properties [5, 7, 19].

In the present work sintering behavior and microstructure development of α/β–SiC-AlN-Y_2O_3 materials under conditions of pressure-less sintering were investigated.

Experimental

Mixtures were prepared from high-purity powders of α–SiC (UF-15, H. C. Starck, Goslar, Germany), β–SiC (B10, H. C. Stark, Goslar, Germany), AlN (H. C. Starck, Germany, grade C), and Y_2O_3 (>99.98 % purity, Aldrich Chemical Company , USA) by attrition milling with alumina milling media in isopropyl alcohol for 4 hours at 500 RPM. The total amount of sintering aids was kept constant at 10 vol.%. The ratio of α–SiC/β–SiC was a variable parameter, the content of α–SiC chosen as 5wt.% and 10 wt.% relative to the amount of β–SiC. The ratio AlN/Y_2O_3 was kept constant at 3:2, the proportion chosen from the AlN – Y_2O_3 phase diagram [20].

The slurry obtained after attrition milling was separated from the milling media by passing through a 320 μm sieve and subsequently dried in a vacuum rotaevaporator. Samples of the mixture were taken for granulometric analysis and specific surface determination. The former was performed by means of laser sedigraphy (Granulometer 1064, CILAS, France), while the latter was accomplished by BET (ASAP 2000, Micrometrics Instrument Corp., USA).The process of drying was then completed in a drying box (48 hours, 65°C). Finally, the powder was passed through a 160 μm sieve to crush soft conglomerates.

Green bodies in the form of cylindrical pellets mm in diameter and mm height were prepared by consequent uniaxial pressing at 100 MPa, and cold isostatic pressing at 200 MPa. Dilatometric experiments were accomplished in a high temperature differential dilatometer (Netzsch GmbH, Germany) with a graphite resistance furnace and working parts in a stagnant argon

atmosphere under normal pressure. Sintering was accomplished in a gas-pressure furnace (Thermal Technologies, Santa Barbara, USA) with a graphite heating element in argon atmosphere.

Sintered samples were characterized for weight loss, density, phase composition and microstructure. Density was determined by Archimedes method. Phase composition was studied by X-ray diffraction (XRD) on a Siemens D-6000 powder diffractometer (Ni-filtered CuKα radiation, range of detection 10-80° 2Θ). Microstructure was studied by scanning electron microscopy (SEM) on a Phillips XL-30 electron microscope with EDS analyzing attachment. Samples for microstructure investigation were prepared by standard ceramographic procedure of multistep grinding and polishing with subsequent chemical etching in a molten NaOH at 400°C for structural elements revelation.

Results and discussion

The nominal formulation of the prepared mixtures together with some of their granulometric characteristics are presented in Table 1.

Table 1. Characteristics of the powder mixtures

Material	α–SiC wt. %	β–SiC wt. %	Y_2O_3 wt. %	AlN wt. %	Grain size distribution			BET (m^2/g)
					d_{10} [μm]	d_{50} [μm]	d_{90} [μm]	
SiC5	4.32	82.13	10.65	2.90	<0.1	0.38	0.99	13.4
SiC10	8.65	77.80	10.65	2.90	<0.1	0.40	1.05	12.93

As it can be noted, the prepared mixtures can be described as having a narrow particle size distribution, and are of submicron fineness, which suggests favorable sintering behavior.

The results of the dilatometric investigations of the densification behavior of the prepared compositions under different sintering atmosphere – flowing nitrogen and flowing argon – are presented in Fig. 1 and 2. In Fig. 1, the linear shrinkage is plotted versus temperature, and in Fig. 2 the shrinkage rate is plotted versus temperature. As it can be seen, the behavior of both compositions is strikingly different depending on the sintering atmosphere.
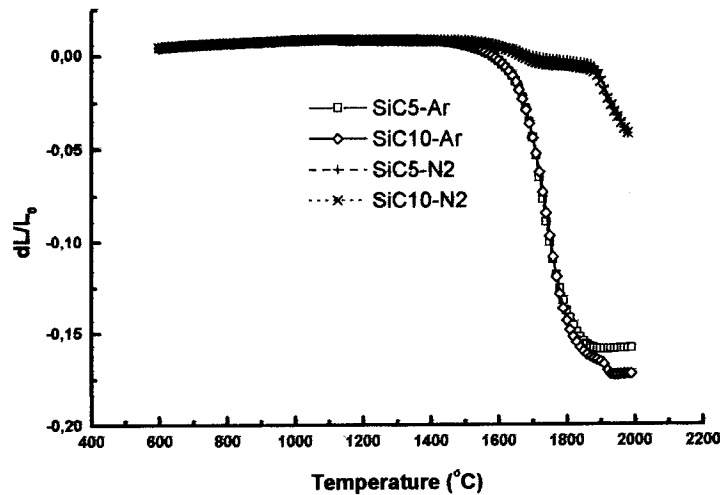

Fig. 1. The results of dilatometric experiments: linear shrinkage vs temperature.
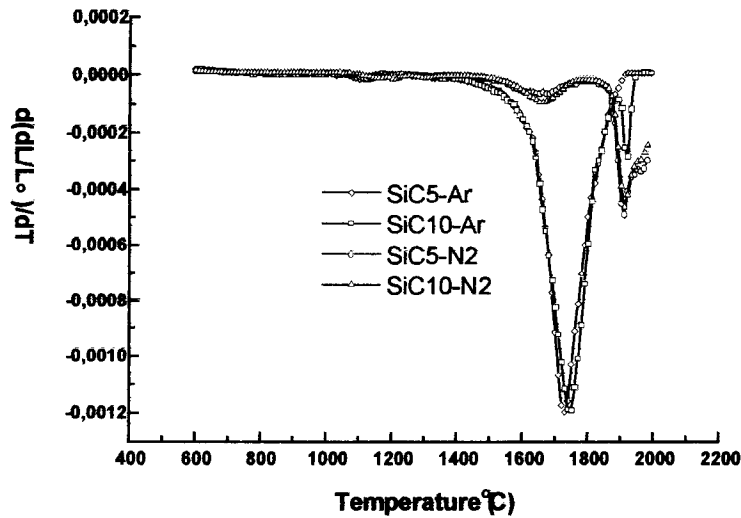
Fig. 2. The results of dilatometric experiments: shrinkage rate *vs* temperature.

It is obvious that nitrogen severely hinders densification in principle. Moreover, the shrinkage rate versus temperature curve has two maximums for both materials, the maximal shrinkage rate corresponding to the temperature of about 1850°C. The first stage of shrinkage, which is more pronounced for the material with 10 wt.% of α-SiC, appears to be rather sluggish and corresponds to the temperature of about 1650°C. If the temperature corresponding to the maximal shrinkage rate is in complete agreement with the AlN-Y_2O_3 phase diagram [20], which shows liquid phase formation for the chosen AlN:Y_2O_3 ratio at about the same temperature, the occurrence of shrinkage at lower temperature can be tentatively explained as a result of the influence of the atmosphere of sintering.

At temperatures exceeding 1420-1430°C, the silica present in the material in the form of surface oxide film on SiC particles, under given atmosphere, and at high partial pressure of carbon-containing gasseous products, can undergo partial nitridation resulting in Si_2N_2O formation. The melting temperature of silicon oxynitride lies at temperatures close to the one of the observed primary shrinkage.

The following decrease of shrinkage until its complete stop can be explained by further nitridation resulting in silicon nitride formation with simultaneous consumption of the oxynitride liquid phase. This supposition is indirectly supported by a formation of a secondary SiC deposit on the surface of the sintered samples. Formation of such a deposit under given thermal conditions and a strongly reductive environment due to a thermal decomposition at higher temperatures of a previously formed silicon nitride with consequent interaction of its decomposition products with carbon-containing species of the sintering atmosphere resulting in secondary deposit SiC formation. However, further experiments are necessary for confirmation of the hypothesis formulated above.

The shrinkage behavior of the same compositions when sintered in argon is quite different. Both the absolute values of linear shrinkage and of the shrinkage rate are sufficiently higher (see Fig. 1 and 2), and the main shrinkage occurs at the temperatures of 1730-1750°C, which is about a

100°C lower than while sintering in nitrogen. This can be explained by the absence of the chemical interaction described above. The occurrence of shrinkage and the shift of the maximal shrinkage rate values to the temperatures predicted by the AlN-Y_2O_3 phase diagram can be explained by the already mentioned presence of SiO_2, which reacts with the sintering additives, AlN and Y_2O_3, and leads to a lower temperature of liquid phase formation, and higher amount of the less viscous liquid phase formed.

The only irregularity observed while sintering in argon was the occurrence of a second stage of shrinkage at about 1850°C, i. e., at the liquid phase formation of the pure AlN – Y_2O_3 sintering additive system, for the composition with 10 wt. % of α–SiC added. Until now no plausible explanation for this effect can be provided, and further experimental work is necessary to elucidate the exact mechanism and sequence of the sintering process of the composition in question. It appears, however, that for this composition some amount of sintering additives were not involved in the primary liquid phase formation and produced a melt only at the liquidus temperature of the AlN – Y_2O_3 system. Based on the size of the second shrinkage rate peak (Fig. 1), it is also possible to presume that the amount of the liquid formed at 1850°C was sufficiently lower and/or that its viscosity was sufficiently higher than that of the primary liquid phase formed earlier, thus resulting only in a limited shrinkage.

Based on the results of the dilatometric investigations the time-temperature sintering schedule for furnace sintering was developed as presented in Fig. 3. The results of the furnace sintering of the prepared compositions in nitrogen and argon are presented in Table 2.

It can be observed that the atmosphere of sintering influences both the weight loss and the final density of the sintered materials. While the weight loss is slightly less in nitrogen atmosphere, the sintered densities are sufficiently lower than the ones achieved during sintering in argon. The increase of the amount of the α–SiC added resulted in a somewhat lower weight loss and a slightly lower final density both in the case of nitrogen and argon as the sintering atmosphere.

Table 2. Green density, sintered density and weight loss after furnace sintering of SiC5 and SiC10 compositions.

Composition	Atmosphere of sintering	Green density % td	Apparent density g/cm^3	Relative density % td	Weight loss %
SiC5	nitrogen	55.1	2.90	86.83	2.70
	argon	55.2	3.25	97.31	3.21
SiC10	nitrogen	55.1	2.86	85.63	2.54
	argon	55.1	3.24	97.01	2.99

Microstructural investigations by SEM of the polished and chemically etched surfaces of the furnace sintered samples showed very different trends in the microstructure formation for the samples sintered in nitrogen and argon of the same materials. Sintering in nitrogen lead to completely inhomogeneous material formation. As it can be seen in Fig. 4(a), where a polished and etched cross-section of a SiC10 sample sintered in nitrogen is shown, a so-called rim structure was formed, i. e., the outer part of the sample was different in color, density, and composition in relation to the bulk of the sample. Moreover, an obvious overall inhomogeneity can be easily seen. According to EDS analysis, the light areas are enriched in Y_2O_3, while the darker areas appear to be Y_2O_3-free. It is obvious that sintering in nitrogen resulted in extremely inhomogeneous secondary phase distribution in the material. The exact mechanism responsible for such an occurrence is not completely clear until now, however, it is quite apparent that the nitrogen atmosphere leads to the alteration of the liquid phase formation process as a whole, most probably influencing the chemical
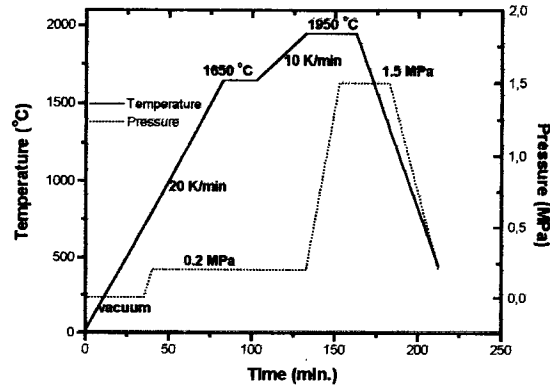
Fig. 3. Time-temperature-pressure schedule of furnace sintering.

composition of the liquid phase, and hence, the phase formation sequence during sintering. These results demonstrate that nitrogen is not a suitable atmosphere for sintering of SiC-AlN-Y$_2$O$_3$ compositions, both in respect of densification and phase- and structure formation.

Microstructural observations of the samples sintered in argon show that materials formed has a homogeneous phase distribution as well as a homogeneous microstructure (see Fig 4(b) and Fig. 5). The influence of α– to β–SiC ratio can be observed on Fig. 5, which shows that the increase of α–SiC content causes the change of the overall grain morphology: with higher α–SiC content the grains have higher aspect ratio, while the microstructure of the material with lower α–SiC content leads to a more uniaxed microstructure. These observations enable to conclude that under conditions of liquid phase sintering of the SiC-AlN-Y$_2$O$_3$ system a transformation-controlled grain growth mechanism, similar to the one established for Si$_3$N$_4$-based ceramics, occurs. This in turn means that all the techniques and approaches for the tailoring microstructure design for the purpose of structural-sensitive properties, such as flexural strength and fracture toughness, premeditated modification which are developed for the silicon nitride based ceramics might be applied to the liquid phase sintered silicon carbide based ceramics.
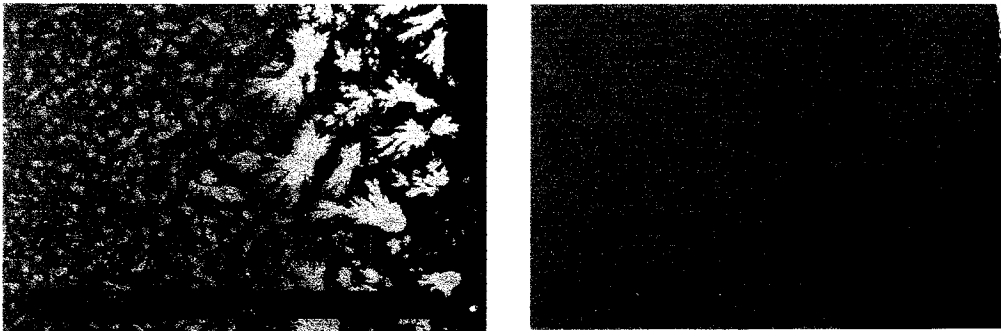

Fig. 4. Polished and chemically etched surface of the (a) SiC5 sample sintered in nitrogen, and (b) of the SiC5 sample sintered in argon under the same time-temperature conditions.
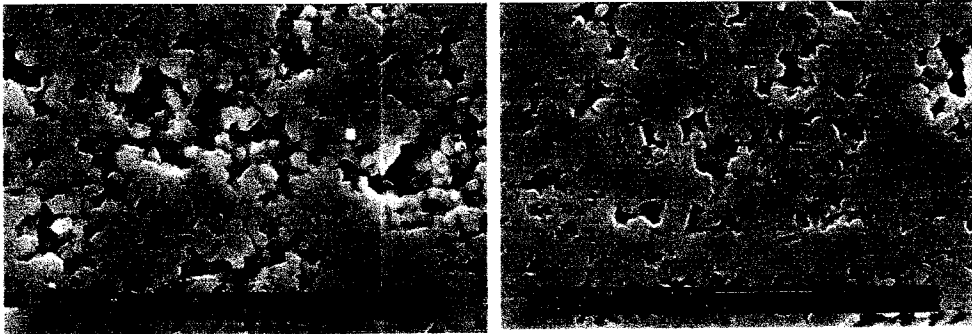
Fig. 5. Microstructure of the (a) SiC5 and (b) SiC10 samples sintered in argon under same conditions.

XRD investigations showed that while the samples sintered in argon have as crystalline phases β–SiC (3C, JCPDF card 29-1128), trace amounts of α–SiC (6H, JCPDF card 29-1131), and trace amounts of a phase that was not identified both on the surface and bulk parts of the samples, the samples sintered in nitrogen had inhomogeneous phase composition.

The surface part of the sample sintered in nitrogen revealed a strong peak of Y_2O_3 (JCPDF card 43-0661), β–SiC, small amount of α–SiC, and a phase tentatively identified as $Y_{10}Al_2Si_3O_{18}N$ (JCPDF card 32-1426), the bulk of the sample contained β–SiC, trace amounts of Y_2O_3 , and trace amounts of unidentified phase. Further experiments on phase composition evolution, specifically α– to β–SiC transformation and secondary phase crystallization during post-sintering heat treatment is planned.

Conclusions

Silicon carbide can be effectively densified up to high densities by means of liquid phase sintering under low gas pressure with AlN and Y_2O_3 sintering additives in argon sintering atmosphere. Materials sintered in argon exhibited fine-grained homogeneous microstructure.

Sintering in nitrogen results in retarded densification and severe inhomogeneity of structure and phase composition.

Increase of the amount of α–SiC in the starting mixtures resulted in slight coarsening of the microstructure and higher aspect ratios of the formed grains. Transformation-controlled grain growth mechanism was established. However, further research must be conducted for elucidating the evolution of the α– to β–SiC phase transformation under conditions of post-sintering heat treatment.

Acknowledgements

References

1. S. Prochaska, The role of boron and carbon in sintering of silicon carbide; pp 171-81 in: *Special Ceramics 6*. Edited by P. Popper. The British Ceramic Research Association, Stoke-on-Trent, U. K., 1975.

2. R. A. Cutler and T. B. Jackson, Liquid phase sintered silicon carbide; pp 309-18, in *Ceramic Materials and Components for Engines*, Proceedings of the Third International Symposium. Edited by V. J. Tennery. American Ceramic Society, Westerwille, OH, 1989.

3. M. A. Mulla and V. D. Krstic, Low-temperature pressureless sintering of β-silicon carbide with aluminum oxide and yttrium oxide additions. Am. Ceram. Soc. Bull., **70** [3] (1991) 439-43.

4. M. A. Mulla and V. D. Krstic, Pressureless sintering of β-SiC with Al_2O_3 additions. J. Mater. Sci., **29** (1994) 934-38.

5. S. K. Lee and C. H. Kim, Effects of α- SiC versus β-SiC starting powders on microstructure and fracture toughness of SiC sintered with Al_2O_3-Y_2O_3 additives. J. Am. Ceram. Soc., **77** [6] (1994)1655-58.

6. M. Omori and H. Takei, Pressureless Sintering of SiC. J. Am. Ceram. Soc., **65** [6] (1982) C-92.

7. P. Padture, In-situ toughening silicon carbide. J. Am. Ceram. Soc., **77** [2] (1994) 519-23.

8. W. J. Kim and Y.-W. Kim. Liquid-phase sintering of silicon carbide. J. Kor. Ceram. Soc., **32** [10] (1995) 1162-68.

9. W. Bocker, H. Landfermann, and H. Hausner, Sintering of α-silicon carbide with additions of aluminium. Powd. Metall. Intern., **11** (1979) 83-85.

10. K. Negita, Effective sintering aids for silicon carbide ceramics: reactivities of silicon carbide with various additives. J. Am. Ceram. Soc., **69** [12] (1986) C-308-C310.

11. K. Y. Chia, W. D. G. Boecker, R. S. Storm, Silicon carbide bodies having high toughness and fracture resistance and method of making same. United States Patent, 5. 298. 470, USA, 1994.

12. M. Keppeler, H.-G. Reihert, J. M. Broadly, G. Turn. I. Wiedmann, and F. Aldinger, High temperature mechanical behavior of liquid phase sintered silicon carbide. J. Eur. Ceram. Soc., **18** (1998) 521-26.

13. R. Ruh, A. Zangvil, Compositions and properties of hot-pressed SiC-AlN solid solutions. J. Am. Ceram. Soc., **65** [5] (1982) 260-65.

14. A. Zangvil, R. Ruh, The $Si_3Al_4N_4C_3$ and $Si_3Al_5N_5C_3$ compounds as SiC-AlN solid solutions. J. Mat. Sci. Lett., **3** (1984) 249-50.

15. A. Zangvil, R. Ruh, Solid solutions and compositions in the SiC-AlN and SiC-BN systems.Mat. Sci. Eng., **71** (1985) 159-64.

16. A. Zangvil. R. Ruh, Phase relationships in the silicon carbide-aluminum nitride system. J. Am. Ceram. Soc., **71** [10] (1988) 884-90.

17. J.-K. Lee, H. Tanaka, S. Otami, Preparation of SiC - AlN composites by liquid-phase sintering and their microstructure. J. Ceram. Soc. Japan, **103** [9] (1995) 873-77.

18. L. S. Singhal, H.-J. Kleebe, Core/rim structure of liquid-phase-sintered silicon carbide. J. Am. Ceram. Soc., **76** (1993) 773-76.

19. L. S. K. Lee, Y. C. Kim, C. H. Kim, Microstructural development and mechanical properties of pressureless-sintered SiC with plate-like grains using Al_2O_3-Y_2O_3 additions. J. Mater. Sci., **29** (1994) 5321-26.

20. A. Jeutter, Untersuchung der Phasenbezieung im Sysytem Aluminiumnitrid-Yttriumoxid. Diplomarbeit an Universitat Stuttgart, (1993).

Advanced Powder Technology II
doi:10.4028/www.scientific.net/KEM.189-191

Liquid-Phase Sintering of SiC-Based Ceramics
doi:10.4028/www.scientific.net/KEM.189-191.173